

GA-A26117

ELM-INDUCED PLASMA WALL INTERACTIONS IN DIII-D

by

**D.L. RUDAKOV, J.A. BOEDO, J.H. YU, N.H. BROOKS,
M.E. FENSTERMACHER, M. GROTH, E.M. HOLLMANN, C.J. LASNIER,
A.G. McLEAN, R.A. MOYER, P.C. STANGEBY, G.R. TYNAN,
W.R. WAMPLER, J.G. WATKINS, W.P. WEST, C.P.C. WONG, R.J. BASTASZ,
D. BUCHENAUER, and J. WHALEY**

NOVEMBER 2008



DISCLAIMER

This report was prepared as an account of work sponsored by an agency of the United States Government. Neither the United States Government nor any agency thereof, nor any of their employees, makes any warranty, express or implied, or assumes any legal liability or responsibility for the accuracy, completeness, or usefulness of any information, apparatus, product, or process disclosed, or represents that its use would not infringe privately owned rights. Reference herein to any specific commercial product, process, or service by trade name, trademark, manufacturer, or otherwise, does not necessarily constitute or imply its endorsement, recommendation, or favoring by the United States Government or any agency thereof. The views and opinions of authors expressed herein do not necessarily state or reflect those of the United States Government or any agency thereof.

ELM-INDUCED PLASMA WALL INTERACTIONS IN DIII-D

by

D.L. RUDAKOV,* J.A. BOEDO,* J.H. YU,* N.H. BROOKS,
M.E. FENSTERMACHER,[†] M. GROTH,[†] E.M. HOLLMANN,* C.J. LASNIER,[†]
A.G. McLEAN,[‡] R.A. MOYER,* P.C. STANGEBY,[‡] G.R. TYNAN,*
W.R. WAMPLER,[¶] J.G. WATKINS,[¶] W.P. WEST, C.P.C. WONG, R.J. BASTASZ,[#]
D. BUCHENAUER,[#] and J. WHALEY

This is a preprint of a paper to be presented at the Eighteenth
International Conference on Plasma Surface Interactions,
May 26-30, 2008, in Toledo, Spain, and to be published in the
J. Nucl. Mater.

*University of California-San Diego, La Jolla, California.

[†]Lawrence Livermore National Laboratory, Livermore, California.

[‡]University of Toronto Institute for Aerospace Studies, Toronto, Canada.

[¶]Sandia National Laboratories, Albuquerque, New Mexico.

[#]Sandia National Laboratories, Livermore, California.

Work supported in part by
the U.S. Department of Energy

under DE-FG02-07ER54917, DE-FC02-04ER54698, DE-AC52-07NA27344,
and DE-AC04-94AL85000

GENERAL ATOMICS ATOMICS PROJECT 30200
NOVEMBER 2008

Abstract

Intense transient fluxes of particles and heat to the main chamber components induced by edge localized modes (ELMs) are of serious concern for ITER. Plasma interaction with the outboard chamber wall is studied in DIII-D using Langmuir probes and optical diagnostics. Fast camera data shows that ELMs feature helical filamentary structures aligned with the local magnetic field. During an ELM, multiple filaments are ejected from the plasma edge and propagate towards the outboard wall with velocities of 0.5-0.7 km/s. Upon reaching the wall, filaments result in regions of local intense plasma-material interaction (PMI) where peak incident particle and heat fluxes are up to 2 orders of magnitude higher than those between ELMs. In low density/collisionality H-mode discharges, PMI at the outboard wall is almost entirely due to ELMs. A moderate change of the gap between the separatrix and the outer wall strongly affects PMI intensity at the wall.

1. Introduction

Limiting plasma-material interactions (PMI) to acceptable levels presents one of the most difficult challenges for next-step fusion devices such as the International Thermonuclear Experimental Reactor (ITER) [1]. The plasma facing components (PFCs) in ITER have to withstand incident fluxes of particles and energy orders of magnitude higher in size and duration than those encountered in present day tokamaks [1]. Though most of the energy and particles crossing the last closed flux surface (LCFS) into the scrape-off layer (SOL) are expected to be transported into the divertor where the PMI is strongest [2], plasma contact with main chamber components is non-negligible. Of particular concern are the impulsive loads due to transient events such as disruptions and edge-localized modes (ELMs) [1,3-11]. Studies at contemporary tokamaks have shown that ELMs can drive a significant portion of the total particle and energy exhaust to main chamber PFCs [6-11]. Moreover, it has been shown that ELMs in the SOL have a filamentary structure [4,6,7,9-11], and individual filaments reaching the main chamber wall can cause localized intense PMI [9,11]. If this happens in ITER, it may cause local melting of beryllium PFCs, leading to enhanced erosion and increased dust production. Sufficiently large gaps between the wall and the separatrix and/or additional protection limiters may be needed to avoid this problem.

2. Structure of the DIII-D Outboard SOL and Diagnostic Arrangement

Figure 1 shows a poloidal cross-section of a typical lower single-null (LSN) equilibrium in DIII-D showing the LCFS and a number of SOL magnetic flux surfaces. There are three distinct regions in the low field side (LFS) SOL [9]: (1) The “Divertor SOL” (DSOL) is the region where magnetic field lines connect from the outboard to the inboard side of the torus, (2) The “Limiter SOL” (LSOL) is the region where both sides of the magnetic field lines terminate on the divertor baffles. In configurations with a large upper gap (UG) and/or small outer wall gap (OWG) the LSOL may not exist. (3) Further radially outwards from the LSOL is the “Outer Wall Shadow” (OWS) region, where magnetic field lines terminate at the outer wall near the midplane. There are three bumper limiters (BLs) [Fig. 2(a)] on the outer wall separated toroidally by approximately 120 degrees and protruding ~ 2 cm inwards from the wall tile radius.

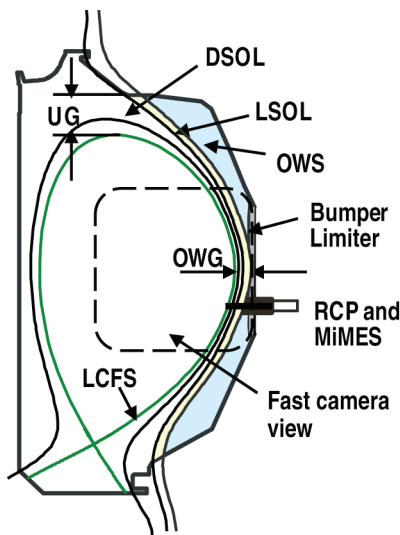


Fig. 1. Diagnostic arrangement and structure of the DIII-D SOL in a LSN magnetic configuration.

Previous studies of plasma interaction with the LFS chamber wall in DIII-D relied almost exclusively on the mid-plane reciprocating probe array (RCP) and a fast profile reflectometer. A number of new diagnostics useful for wall PMI studies have recently been commissioned. A fast framing CMOS camera (Phantom 7.1) with a tangential view of the outboard chamber wall and spatial resolution of about 5 mm has been successfully used [11]. Two new filterscopes (telescopes with spectral line filters coupled to photomultipliers) have been installed, one with a view of a mid-plane portion of a bumper limiter and another with a view of the wall tiles nearby [Fig. 2(a)]. In addition, the capability to install material samples at the outer shield of the RCP (Midplane Material Evaluation Station or MiMES) has been recently

implemented. This allows *in-situ* measurements of net erosion/deposition at the LFS chamber wall. Samples can be exchanged through an airlock. A photograph of MiMES inside the airlock chamber is shown in Fig. 2(b).

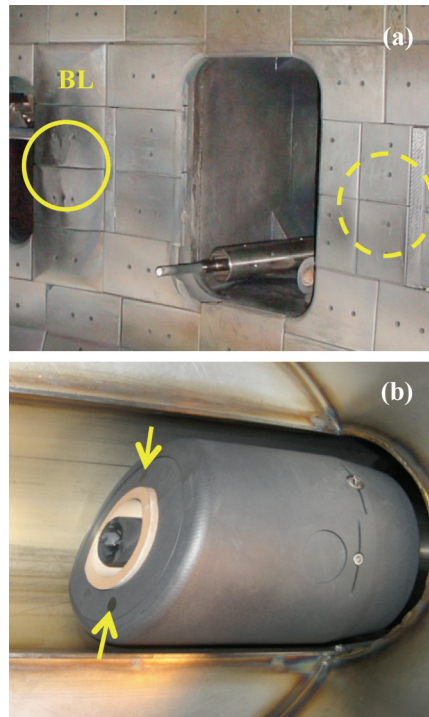


Fig. 2. Photographs of (a) portion of LFS chamber wall showing a bumper limiter (BL), view spots of the BL (solid circle) and wall (dashed circle) filterscopes, and mid-plane RCP with the outer shield removed; (b) RCP with MiMES inside the airlock chamber. Locations of depth-marked graphite button samples are marked by arrows.

3. Experimental Results

ELM propagation through the LFS SOL and interaction with the outboard wall were studied in LSN H-mode discharges with the following parameters: toroidal magnetic field, $B_T = 1.7\text{--}2.1$ T, plasma current, $I_p = 1\text{--}1.4$ MA, neutral beam heating power, $P_{NBI} = 1.5\text{--}7$ MW, line-average plasma density, $\bar{n}_e = 0.5\text{--}1.2 \times 10^{20}$ m⁻³, density normalized to Greenwald limit, $f_{GW} \equiv n_e/n_{GW} = 0.35\text{--}1$.

Fast camera data shows that ELMs in the LFS edge and SOL feature helical filamentary structures aligned with the local magnetic field. Figure 3(a,b) shows ELM filaments imaged in CIII light (465 nm) in low [(a), $f_{GW} = 0.35$] and moderate [(b), $f_{GW} = 0.7$] density discharges. Toroidal mode number, n , increases with discharge density from 10–20 in the low-density case to over 30 at higher density [11]. During the nonlinear phase of an ELM, multiple filaments are ejected from the plasma edge and propagate radially outwards through the SOL. These observations are consistent with the previous probe measurements showing that ELMs in the SOL have fine structure with multiple bursts of ion saturation current measured during each ELM [3,5-7,9]. The filament radial propagation velocity is estimated from the camera data to be 500 ± 400 m/s, and is consistent with the $E \times B$ velocity of ~ 700 m/s inferred from the probe data [6,7] and the ELM density pulse propagation velocity of ~ 500 m/s as estimated from reflectometer data [3]. Upon reaching the wall, the filaments cause PMI that is clearly observed in D_α (656 nm) emission [Fig. 3(c,d)] due to release of neutrals from the wall tiles. Localized areas of intense PMI are observed in both the low and moderate density cases, however, in the lower density

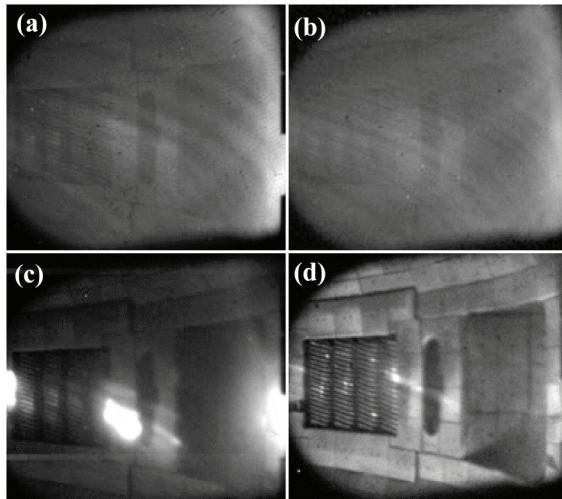


Fig. 3. Fast camera images of ELM filaments in CIII light near the separatrix (a,b), and in D_α light interacting with the outboard wall (c,d), in low (a,c) and moderate (b,d) density discharges.

case their relative brightness is much larger. This is consistent with an earlier conclusion made from the probe data that the relative contribution of the ELMs to the (parallel) particle flux arriving at the outboard wall decreases from 80%-90% at $f_{GW} = 0.4\text{--}0.5$ to about 30% at $f_{GW} \sim 1$ [9]. Figure 4 shows results of similar analysis applied to the parallel heat flux, $q_{||} = 7kT_e j_{si}/e$, where T_e is the electron temperature and j_{si} is the ion saturation current density measured by the probe near the outer edge of LSOL. A similar trend is observed, but the relative contribution of ELMs to the net local heat flux is somewhat higher compared to the particle flux.

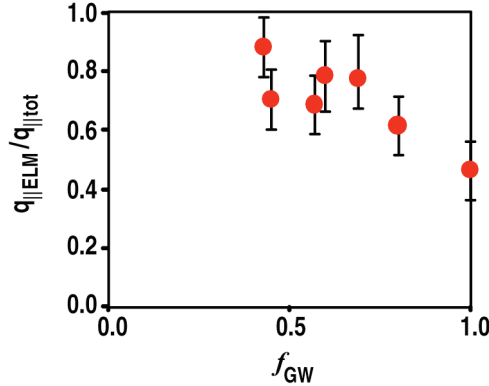


Fig. 4. Relative contribution of ELMs to the local parallel heat flux at the outer edge of the LSOL as a function of the normalized discharge density.

While propagating through the SOL, ELM filaments are depleted of particles and energy by parallel losses, and may partially or fully decay before reaching the wall [6,7,9]. This is illustrated in Fig. 5 showing radial profile of the peak ion saturation current, I_{si} , within ELM filaments (squares) measured by the RCP in the far SOL of a high-density ($f_{GW} \sim 1$) discharge. This discharge had a large upper gap (9.3 cm) and no LSOL. Within a radial distance of ~ 4 cm shown in the plot, the filament amplitude decays by almost two orders of magnitude. Throughout the region shown it remains about 10X greater than the inter-ELM background (diamonds). Later in the discharge, the outer wall gap was transiently reduced by 3 cm [Fig. 6(a)]. This resulted in increases in both filament amplitude and background density in the DSOL and throughout most of the OWS region [Fig. 5(b)]. The BL and wall filterscopes evidenced increased PMI at the LFS wall manifesting itself by an increase in D_α emission [Fig. 6(b), BL filterscope signal from a similar discharge shown]. In subsequent discharges the wall gap was transiently increased by 3 cm resulting in ~ 4 reduction of the peak D_α emission during ELMs. Thus a moderate change of the OWG has a significant effect at the level of plasma interaction with the LFS wall.

Graphite button samples installed on the plasma-facing side of MiMES [Fig. 2(b)] were exposed in seven high-density H-mode discharges similar to those illustrated in Figs 5 and 6. During the exposure, the samples were in the OWS (~ 0.5 cm outside of the DSOL border) for a total of ~ 16 plasma-seconds and in the DSOL (~ 1.5 cm inside of OWS border) for ~ 12 plasma-seconds. The samples were implanted with a Si

depth marker that allowed measurement of net erosion/deposition by ion beam analysis (IBA) (in progress at Sandia National Laboratories, Albuquerque). The RCP was fixed during the exposure so that the tips measuring I_{Si} were ~5 mm inwards of the sample location, as shown in Fig. 2(b). During OWG scans, I_{Si} measured by the probe behaved similarly to D_{α} emission measured by BL and wall filterscopes [Fig. 6(c)].

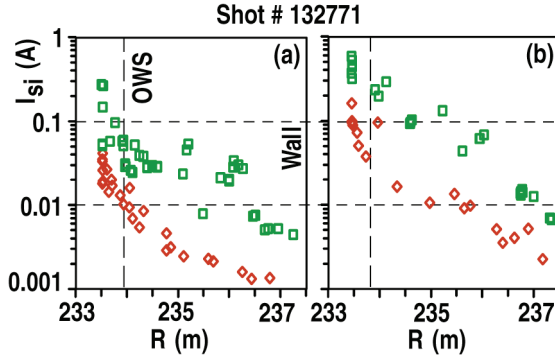


Fig. 5. Radial profiles of the peak I_{Si} within ELM filaments (squares) and between-ELM background (diamonds) in the far SOL of a high density ($f_{\text{GW}} \sim 1$) LSN discharge with an OWG of 9.3 cm (a) and 6.3 cm (b).

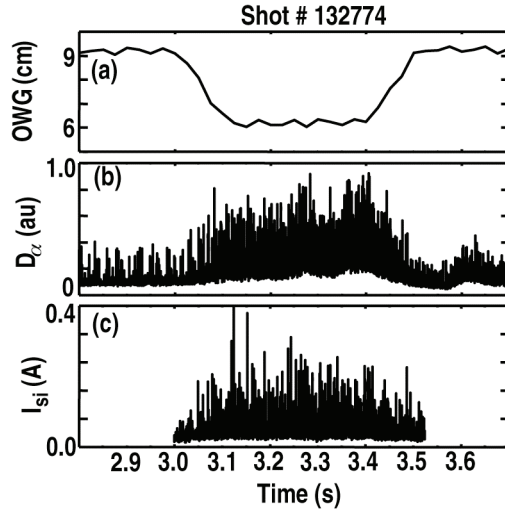


Fig. 6. Changes in outer wall PMI with decreased outer wall gap (a). Shown are D_{α} emission measured by BL filterscope (b) and I_{Si} to a probe fixed at the LSOL/OWS boundary (c).

4. Summary and Conclusion

Experimental evidence showing that ELMs cause significant plasma interaction with the main chamber wall in DIII-D has been presented. The relative contribution of ELMs to PMI with the LFS chamber wall decreases with increasing discharge density, which, in DIII-D, is coupled to increasing pedestal collisionality. Since ITER will have high-normalized density and low collisionality, it is not clear how large the relative importance of ELMs for the main chamber PMI will be. Even at high density close to the Greenwald limit, ELM filaments may reach the LFS wall and cause erosion of the wall tiles. A moderate increase of the gap between LCFS and the wall may decrease PMI intensity appreciably. Therefore, if ELM interaction with the main chamber wall is determined to be a challenge for ITER, provision for an increased wall gap may be extremely advantageous.

References

- [1] G. Federici, *et al.*, Nucl. Fusion **41** (2001) 1967.
- [2] P.C. Stangeby, *The Plasma Boundary of Magnetic Fusion Devices*, IOP Publishing, 2000.
- [3] M.E. Fenstermacher, *et al.*, Plasma Phys. Control. Fusion **45** (2003) 1597.
- [4] A. Kirk, *et al.*, Phys. Rev Lett. **92** (2004) 245002.
- [5] D.L. Rudakov, *et al.*, J. Nucl. Mater. **337-339** (2005) 717.
- [6] J.A. Boedo, *et al.*, J. Nucl. Mater. **337-339** (2005) 771.
- [7] J.A. Boedo, *et al.*, Phys. Plasmas **12** (2005) 072516.
- [8] D.G. Whyte, *et al.*, Plasma Phys. Control. Fusion **47** (2005) 1579.
- [9] D.L. Rudakov, *et al.*, Nucl. Fusion **45** (2005) 1589.
- [10] B. Lipschultz, *et al.*, Nucl. Fusion **47** (2007) 1189.
- [11] J.H. Yu, *et al.*, Phys. Plasmas **15** (2008) 032504.

Acknowledgment

This work was supported by the US Department of Energy under DE-FG02-07ER54917, DE-FC02-04ER54698, DE-AC52-07NA27344, and DE-AC04-94AL85000.